

Field validation of a free-agent cellular automata model of fire spread with fire–atmosphere coupling

Gary L. Achtemeier

Center for Forest Disturbance Science, USDA Forest Service, Athens, GA, 30602, USA.
Email: gachtemeier@fs.fed.us

Abstract. A cellular automata fire model represents ‘elements’ of fire by autonomous agents. A few simple algebraic expressions substituted for complex physical and meteorological processes and solved iteratively yield simulations for ‘super-diffusive’ fire spread and coupled surface-layer (2-m) fire–atmosphere processes. Pressure anomalies, which are integrals of the thermal properties of the overlying heated plume, drive the surface winds around and through the fire. Five simulations with differing fuel and wind conditions were compared with fire and meteorological data from an experimental grassfire (FireFlux). The fire model accurately simulated bulk patterns of measured time-series of 2-m winds at two towers and observed fire behaviour (spread rate, flaming depth and heat released). Fidelity to spatial windfields in the vicinity of the fire was similar to results from full-physics fire models for other grassfires. Accurate predictions of fire spread depend critically on accurate wind speeds and directions at the location of the fire. Simulated fire–atmosphere coupling using FireFlux data increased wind speeds across the fire line by up to a factor of three. With its computational speed relative to full-physics models, the fire model can inform full-physics modellers regarding problems of interest. Although the fire model is tested for homogeneous fuels on flat terrain, the model is designed for simulating complex distributions of fire within heterogeneous distributions of fuels over complex landscapes.

Received 23 April 2011, accepted 3 July 2012, published online 25 September 2012

Introduction

Numerous fire models have been developed for predicting fire spread and providing operational tools for land managers. Linn *et al.* (2007) and Sullivan (2009a) summarised physics-based fire models that can explain mathematically how combustion processes in heterogeneous fuels under variable atmospheric conditions translate to fire behaviour and thence to fire spread (Clark *et al.* 1996; Linn 1997; Linn and Harlow 1998). Sullivan (2009b) summarised empirical-statistical models that link wind, fuel moisture and fire spread.

Cellular automata (CA) are another promising methodology for fire modelling. Each cell of a regular grid representing a landscape contains data on fuel characteristics and terrain. Fuel in combustion in one cell transfers thermal energy (Rothermel 1972) to fuel in adjacent cells. Spread rate is a function of rate of ignition as fire spreads over the landscape. CA models of fire spread (Bouchaud and Georges 1990; Clarke *et al.* 1994; Clarke and Olsen 1996; Karafyllidis and Thanailakis 1997; Metzler and Klafter 2000; Berjak and Hearne 2002; Sullivan and Knight 2004; Hernández Encinas *et al.* 2007; Yassemi *et al.* 2008; Adou *et al.* 2010) have achieved success in modelling fire spread rate as a function of fuels, terrain and weather. CA modelling of fire spread by convective spotting (fire jumps beyond adjacent fuel cells) has been achieved through ‘super-diffusive’ fire models (Bouchaud and Georges 1990; Metzler and Klafter 2000; Sullivan and Knight 2004; Adou *et al.* 2010).

A (CA) fire model (Achtemeier 2003) that simplifies the fire problem through representing ‘elements’ of fire by autonomous

agents (Flakes 2000, p. 261) is the subject of this paper. The model includes rules for coupled fire–atmosphere processes. The CA fire model has been designated ‘Rabbit Rules’. Rabbit Rules advances the methodology for calculating the effect of winds on fire put forth by Sullivan and Knight (2004) so that coupled fire–atmosphere winds approach the complexity of 2-m winds found in full-physics models (Clark *et al.* 1996; Linn and Cunningham 2005).

The model development is presented below, followed by comparisons between model simulations and observations of fire and weather taken during the FireFlux experimental grassfire (Clements *et al.* 2007).

Materials and methods

Fire spread model

The purpose of the autonomous agent is to reduce the complexity of modelling fire while minimising commensurate loss of explanatory power. Therefore, the agent should not be too much like fire or else modelling complexity will not be reduced, nor should the agent be too little like fire or else there will be too little explanatory power. Furthermore, it is assumed that the mechanisms for fire spread can be represented by spotting. A rabbit (the animal) is an appropriate proxy for fire spread by spotting because of a fundamental similarity in behaviours. For example, fire consumes fuel, fire ‘leaps’ from fuel element to fuel element and fire spreads. By comparison, rabbits eat, rabbits jump and rabbits reproduce.

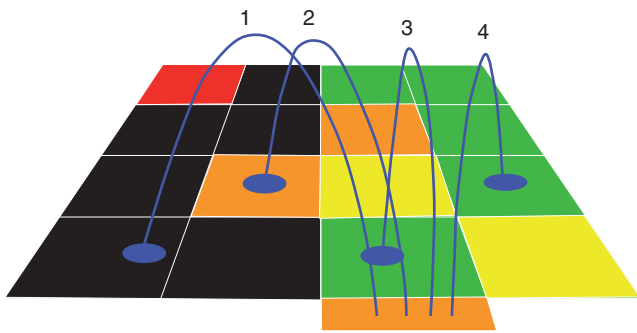


Fig. 1. Hopping paths of four rabbits birthed at the lower extension (orange) of the cellular grid. Yellow cells are occupied by baby rabbits, orange cells are occupied by reproductive rabbits and red cells are occupied by old, declining rabbits. Green cells represent uneaten food and black cells represent eaten food.

Table 1. User-defined coefficients required for Rabbit Rules for tall grass (fn01)

Coefficient	Coefficient definition	Value
m_1, m_2, m_3, m_4	lifespan (min)	0.1, 0, 0, 0
f_h	effective height of fuels (m)	1.0, 1.25, 1.5 (see text)
C_{w0}	wind weight (non)	0.25
C_h	isotropic hopping weight (non)	0.5
C_f	terrain fear factor (non)	1.0
v_g	pressure anomaly (non)	2.0, 2.5, 3.0 (see text)

The fire spread problem is reduced to finding (a) when a rabbit will jump, (b) how far the rabbit will jump and (c) how long a rabbit will live. The physical domain is converted into a fine mesh regular grid with each grid cell given a fuel type number linked to an array of fuel designations. Regarding (a), the rabbit jumps only once at birth. If it lands on an unoccupied food square (green cell in Fig. 1), it survives and passes through the remaining life cycle – adolescent or reproductive (shown by the orange squares) and old or dying (red squares). The reproductive period is the time elapsed after initial landing until new rabbits are launched towards nearby food cells. This period is a function of the size of the food square (defined internally in the model) and the fuel designations and must be linked with empirical data on fire spread (Andrews *et al.* 2005).

Regarding (b), the hopping distance is given by:

$$\begin{aligned} x &= (C_w u |u| + 10 C_f s_x |s_x|) t + C_h z_r (0.5 - ran) \\ y &= (C_w v |v| + 10 C_f s_y |s_y|) t + C_h z_r (0.5 - ran) \end{aligned} \quad (1)$$

The first and second terms in parentheses represent the local spread of burning fuel elements by the east–west (x) and north–south (y) components of the wind (u, v) with a correction factor for slope (s_x, s_y). The third term gives background spread in the absence of wind and slope and z_r is the rabbit hopping height. A random number ($0 < ran < 1$) adds stochasticity to the hopping distance. Each term enters its equation via its respective weight ($C_w, m^{-1} s$; $C_f, m^{-1} s^{-1}$; C_h , non-dimensional) (Table 1).

Thus, in the absence of slope (as in this study), the hopping distance is proportional to the product of the wind speed with the time the rabbit is airborne. The airborne time t (not the same as the reproductive period) is the time elapsed for the rabbit to complete a hop:

$$t = 2 \sqrt{\frac{2 \times z_r}{g}} \quad (2)$$

where the acceleration of gravity $g = 9.81 \text{ m s}^{-2}$. The hopping height, analogous to ember (or firebrand) discharge height, is a simple function of a characteristic fuel height f_h that carries information regarding actual fuel height and fuel moisture:

$$z_r = 2(0.1 + ran) f_h \quad (3)$$

where ran is a random number between zero and one that gives a stochastic component to the hopping height. Should fuel moisture increase, f_h is decreased, hopping height is less, and fire spread rate is reduced.

Finally, Eqn 1 must be multiplied by a constant of proportionality that is solely a function of fuel cell width. The constant is calculated internally in the model and the relationship with fuel height and wind is presented in more detail in reference to rabbit lifetime described below.

Regarding (c), the rabbit survives only if it lands on an empty uneaten food cell (Fig. 1). Landing on all other cells – cells eaten by other rabbits (black), occupied by other rabbits (orange or red), or non-food cells (other non-green colours) – is fatal. Then its longevity, a function of fuel characteristics that include mass and heterogeneity, is assigned through five time coefficients shown as m_1 – m_5 in Table 1. Specified in units of minutes, for rabbits of a particular fuel type, 100% live through m_1 , 50% live through m_2 , 20% live through m_3 , 5% live through m_4 and 1% live through m_5 . The first cutoff defines the residence time of the fire front as it passes through fuel beds. The remaining cutoffs define the number of old or dying rabbits that represent residual burning. The role of rabbit longevity is described in reference to Rule FA1 below.

Eqns 1, 2 and 3 describe a simple CA model for ‘rabbits’ hopping over a landscape. The relationship to fire spread rate (ROS) is analogous: fire spreads faster in stronger winds – rabbits hop farther in stronger winds; fire spreads faster uphill than downhill – rabbits prefer to hop uphill rather than downhill; fire spreads faster when embers fall farther from the fire line – rabbits jump higher, hence get carried farther by the wind, subject to food (fuel) characteristics.

The three rules are linked by weights yet to be determined. Once the characteristic fuel height is set, the relationship between fire spread rate, wind and slope is linear. Therefore, Eqn 1 cannot represent non-linear dependencies present in a general wildland fire and is thus a departure from simulations based on physics-based models. Nonlinear fire–atmosphere coupling is done through secondary rules, FA1 and FA2.

Rule FA1 posits that each rabbit throughout its lifetime discharges a plume of heated air that drifts downwind from the rabbit location. This plume of warm air creates a hydrostatically induced low pressure area at the ground that is too weak to

influence the local winds. However, when summed over a large number of rabbits, the low pressure area can be sufficient to affect the local wind field. Thus Rule FA1 defines how temperature anomalies within the plume of ascending hot gases modify surface air pressure to draw the wind field around and through the fire. Each rabbit is assigned a number (n_p) of pressure anomaly 'points' that define a plume downwind from the rabbit. The location of the n th point relative to the rabbit is:

$$d_n = c_{pn}U(ran)^2 \quad (4)$$

where U is the vector mean wind for the layer containing the heat plume and c_{pn} ($c_{pn} = 0.2, 0.5, 1.0; n_p = 3$) are distance weights normalised to the grid. Use of the square of the random number forces d_n to concentrate closer to the fire thus making Eqn 4 a proxy for heated air within the plume with the hottest air being located just downwind from the fire. The total pressure anomaly at each point of an overlying meteorological grid is the sum of all of the pressure anomalies over all rabbits n_{rab} within a specified distance of that grid point:

$$P_{i,j} = P_{0i,j} + 10^{-4} \sum_{k=1}^{n_{rab}} \sum_{n=1}^{n_p} \delta_{A1} v_{gk} \quad (5)$$

where $\delta_{A1} = 1$ if d_n is located within half a grid space of $P_{i,j}$ else $\delta_{A1} = 0$. $P_{0i,j}$ is a reference pressure here set to 100 kPa. The parameter v_g weights the rabbit 'vigour' according to the fuel type consumed. Thus certain cells may hold fuel types and characteristics that produce more or less heat than at other cells. The summation is multiplied by 10^{-4} to render v_g to the order of one.

Air accelerated through the fire line must be replaced by 'draw-in' of air from behind. Rule FA2 posits that a fraction of the air drawn in comes from aloft. The depth of the layer through which a fire draws, and the intensity of the draw-down, is directly proportional to the strength of the fire. Rule FA2 is the mechanism for downward momentum transport in Rabbit Rules. To avoid vertical momentum transport in divergence not associated with the fire, the draw-down is made a function of the fire-induced pressure anomalies. The quantitative measure for the strength of the draw-down (I) is the Laplacian of the pressure anomaly produced by Rule FA1:

$$I = -\delta_{A2} C_{A2} \nabla^2 P \quad (6)$$

where $\delta_{A2} = 1$ if the Laplacian of pressure is negative else $\delta_{A2} = 0$. C_{A2} scales the draw-down to the order of other rules. Eqn 6 is placed in the meteorological model as a forcing term proportional to the vertical wind shear within the surface layer. For this study, the vertical shear is the difference between the vector winds at 100 and 2 m.

Birth time and number of rabbits birthed are the key links to fire spread rate. Using four as the number of rabbits birthed keeps the solution from fragmenting (Hargrove *et al.* 2000) while controlling computational overload. However, there exist a finite number of fuel cells to which a rabbit can jump. Birthing many rabbits increases computational load without improving model accuracy because most will perish for lack of empty unneaten fuel cells.

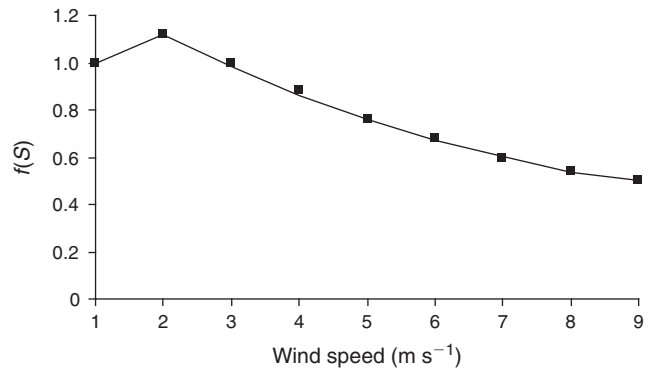


Fig. 2. Correction function for C_w needed to bring fire spread rates in Rabbit Rules in line with spread rates calculated by Andrews (2008).

The above rules and associated steps complete the fire model part of Rabbit Rules. Additional and more complex rules could refine the model. However, model development has been based on simplicity until further research identifies the need for additional rules. Analogous to other cellular automata fire models (Hargrove *et al.* 2000; Berjak and Hearne 2002; Adou *et al.* 2010), a set of parameters must be specified before model execution. The values for characteristic food height, wind, isotropic hopping and vigour (f_h, C_w, C_h, v_g) were assigned by 'training' the rabbits through ~ 200 model runs to match the rate of spread through tall grass over the full range of wind speeds ($0.0-9.3 \text{ m s}^{-1}$) reported by (Andrews 2008). f_h was assigned a value of 3 m for tall grass. C_h was set to 0.5, which was just sufficient to carry fire in calm winds. v_g and C_f were set to zero and Rule FA2 was turned off. Coefficient values were chosen so that fuel height approximated tall grass. Then a relationship between ROS and wind speed was sought for fuel cell sizes over the range from 0.19 to 3.55 m considered typical for running Rabbit Rules for prescribed fire. There was found no functional relationship with fuel cell size. The outcome was a correction function (Fig. 2) for $C_w = C_{w0}f(S)$ where S is the wind speed. Thus:

$$f(S) = 0.01068 \times S^2 - 0.21 \times S + 1.53 \quad (7)$$

if $S > 2.0 \text{ m s}^{-1}$. (See Sullivan (2009b) for a table of wind functions developed for empirical fire spread models.)

Meteorological interface model

The above-derived fire model is embedded within a simple vertically integrated high-resolution semi-Lagrangian meteorological 'interface' model modified from a shallow-layer wind model (Achtemeier 2005). The interface model links the CA fire model with selected output from mesoscale numerical weather prediction models (Grell *et al.* 1994; and Skamarock *et al.* 2005). However, in flat terrain and uniform weather for a relatively small burn area (such as FireFlux), Rabbit Rules can be initialised with local wind observations at 2 and 100 m.

The minimum grid resolution of the interface model is fixed by the US Geological Survey 30-m digital elevation database (<http://seamless.usgs.gov/>, accessed 23 August 2012). Therefore, the wind model cannot resolve circulations on the scale of

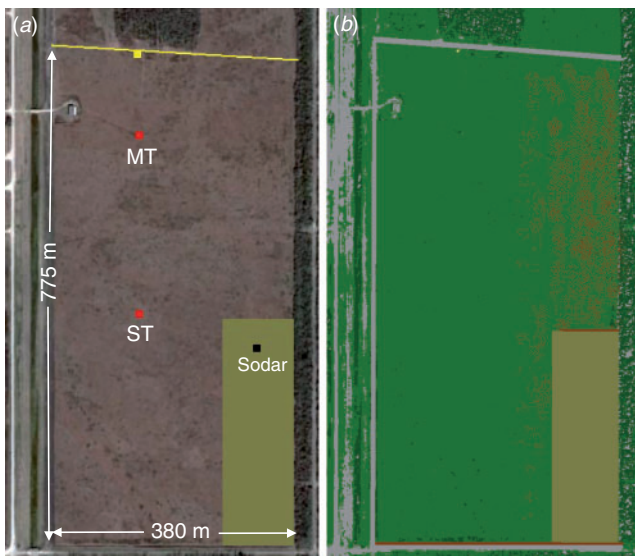


Fig. 3. Specifics of the FireFlux site: (a) the locations of the main and south towers (red squares), the Doppler sodar (black square) and the point of ignition (yellow square) overlain on a Google Earth map. (b) A fuels map showing area to be burned in Rabbit Rules.

the fire but can resolve the bulk circulations initiated by heat flowing through the smoke plume.

Fuels and weather data

The FireFlux experimental fire took place on 23 February 2006 on 155 acres (0.63 km^2) of native prairie in south-eastern Texas $\sim 45 \text{ km}$ south-east of Houston ($29^\circ 23' 16.4'' \text{ N}$, $95^\circ 02' 29.0'' \text{ W}$) (Clements *et al.* 2007). Fig. 3a shows site locations pertinent to this study: the locations of the main (43 m) and south (10 m) towers (red squares), the Doppler sodar (black square) and the point of ignition (yellow square) overlain on a Google Earth map. (See Clements *et al.* for a full description of the instruments used during FireFlux.) The beige-green area enclosing the Doppler sodar site identifies a fire exclusion area where the grass had been previously cut. The area burned was included within a larger meteorological grid (resolution = 30 m) that extended 180 m to the left (west) and 150 m to the right (east) of the field boundaries.

Clements *et al.* (2007) also gave a species description of the tall-grass prairie. Some of the grass reportedly stood at shoulder height (S. A. Goodrick, pers. comm.), or $\sim 1.5 \text{ m}$ high. Fig. 3b shows the fuels map deduced from a colour identification scheme in Rabbit Rules applied to the image in Fig. 3a. No description of fuel height among the various grass species was provided; the fuels were designated as uniform, assigned a single colour and matched with fn01 in Table 1. In addition, grasses described as sparsely spread over the eastern part of the area (Clements, pers. comm.) were 'thinned' in Fig. 3a by using the spray feature in Microsoft Paint. This is a reasonable approximation, commensurate with the other assumptions and approximations in the model.

High-frequency weather data for this study consist of time-series of 1-s temperature, u-component and v-component at 2-m height on both the main and south towers. The temperature data

were used to identify the time of fire passage at each tower. In addition, the Doppler sodar provided vertical wind profiles at 10-min intervals beginning at 40 m above ground level.

Rabbit Rules was initialised with local wind observations at 2 and 100 m. The 2-m wind data as used here are a 1.5-min average of the wind time-series taken at the main tower (005° at 3.25 m s^{-1}) or by a 2.5-min average of the wind time-series taken at the south tower (016° at 4.5 m s^{-1}). The slower winds observed at the main tower were likely the outcome of the obstacle created by a grove of trees located just north of the ignition line (Fig. 3a). The 100-m wind data are provided by the winds measured by the Doppler sodar at 1230 hours LST (017° at 7.7 m s^{-1}).

The fire was ignited at 1243:40 hours at the yellow square in Fig. 3a. Burn crews carrying ignition torches walked in opposite directions from the ignition point along the yellow line. Walking speed was estimated at between 0.5 and 1.0 m s^{-1} (S. A. Goodrick, pers. comm.). Rabbit Rules was stopped every 30 s and a small line segment of 'fire' was added until the torch carriers reached the far eastern edge of the field in 6 min, an average walking speed of 0.67 m s^{-1} .

Results

Validation of Rabbit Rules is limited by the models and the FireFlux dataset. The simple vertically integrated meteorological interface model restricts validation to the surface layer. The 30-m grid resolution requires the fire to cover a sufficiently large area before rules FA1 and FA2 fully affect the wind field.

The validation proceeds in three ways. First, simulated ROS and associated time-series of wind behaviour preceding, during and after fire passage and at the location of two towers were compared with measured fire spread and observed winds at 2 m at both towers. Second, simulated fire line depth and fire intensity were compared with FireFlux tower data. Third, spatial wind fields generated by Rabbit Rules as the simulated fire spread over the FireFlux experimental area were compared with surface-layer winds developed in full-physics fire models for similar grassfires.

Comparisons with FireFlux: fire spread rate and time-series of wind

With the fire residence time for grass set for 0.1 min (6 s) (Table 1), Rabbit Rules was run for various combinations of effective fuel height and pressure anomaly weight (v_g) assigned for each rabbit in Eqn 5. As ROS is tightly linked to wind speed, the time-series of the coupled fire-atmosphere winds should approach the time-series of the winds observed at the two towers as the simulated ROS approaches the observed fire spread rate. The simulated ROS was calculated by locating the leading edge of the front of rabbits every 30 s and dividing by the distance covered.

Fig. 4 shows five simulations that produced ROS near the observed spread rate of 1.33 m s^{-1} between the main and south towers. The observed ROS was defined as the difference between fire arrival times identified by steep rises in temperature (Figs 5a, 6a) divided by the distance between the two towers.

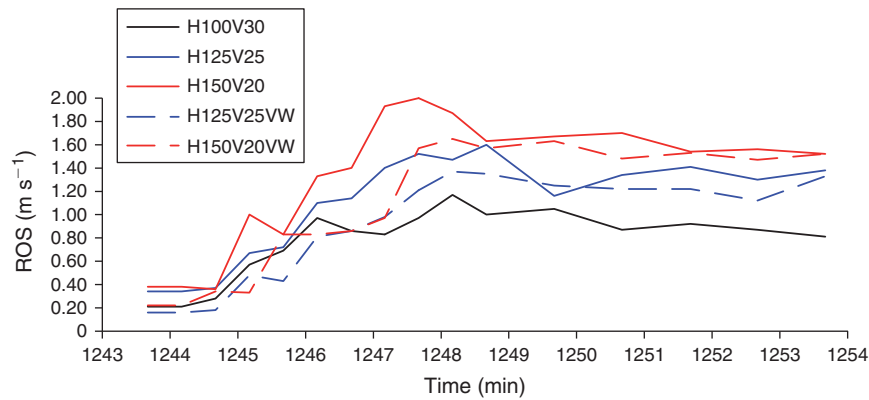


Fig. 4. Spread rates for three simulations with fixed 2-m winds (solid lines) and for two simulations with variable 2-m winds (dashed lines) for the FireFlux burn. In this figure, the 'V' appearing in the legend represents the pressure parameter (v_g) in Eqn 5.

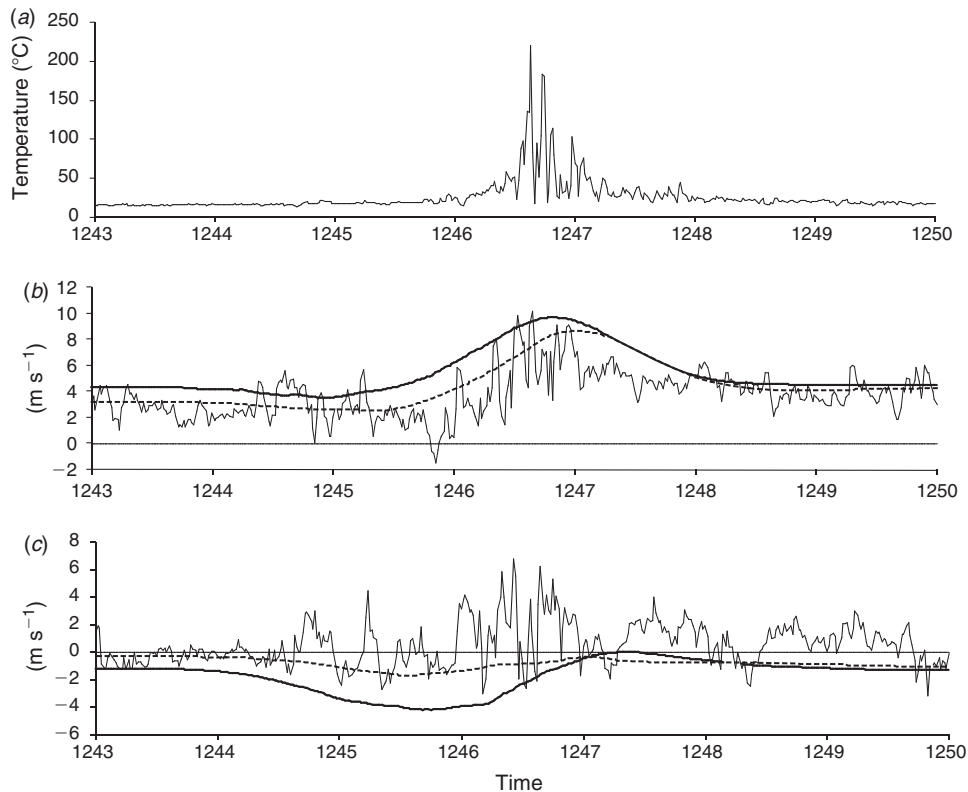


Fig. 5. For the main tower at 2 m: time-series of 1-s averaged (a) temperature, (b) wind u-component and (c) wind v-component overlain with 1-s time-series of the respective wind components obtained via Rabbit Rules for constant wind (solid line) and variable wind (dashed line).

All runs ramp up from slow (less than 0.40 m s^{-1}) spread rates to peak near 1248:00 hours. Run H100V30 (fuel height = 1.0 m ; $v_g = 3.0$) produced a maximum ROS of 1.17 m s^{-1} , but most spread rates remained below 1.00 m s^{-1} . Run H125V25 (fuel height = 1.25 m ; $v_g = 2.5$) peaked at 1.52 m s^{-1} and H150V20 (fuel height = 1.50 m ; $v_g = 2.0$) produced a maximum ROS of 2.00 m s^{-1} . These three simulations (solid lines) were done using ambient 2-m winds from the south tower averaged before the winds were affected by the fire.

Runs H125V25 and H150V20 were repeated with the 2-m wind set for the main tower (005° at 3.25 m s^{-1}). Then, when the fire passed the main tower, the 2-m wind was set for the south tower (016° at 4.5 m s^{-1}). The interface model took $\sim 2 \text{ min}$ to bring the wind to the speed observed at the south tower. Therefore the spread rates from these two variable wind (designated 'VW') simulations (dashed lines in Fig. 4) were generally less in comparison with the runs initialised by the south tower winds but generally converged towards the end of the simulations.

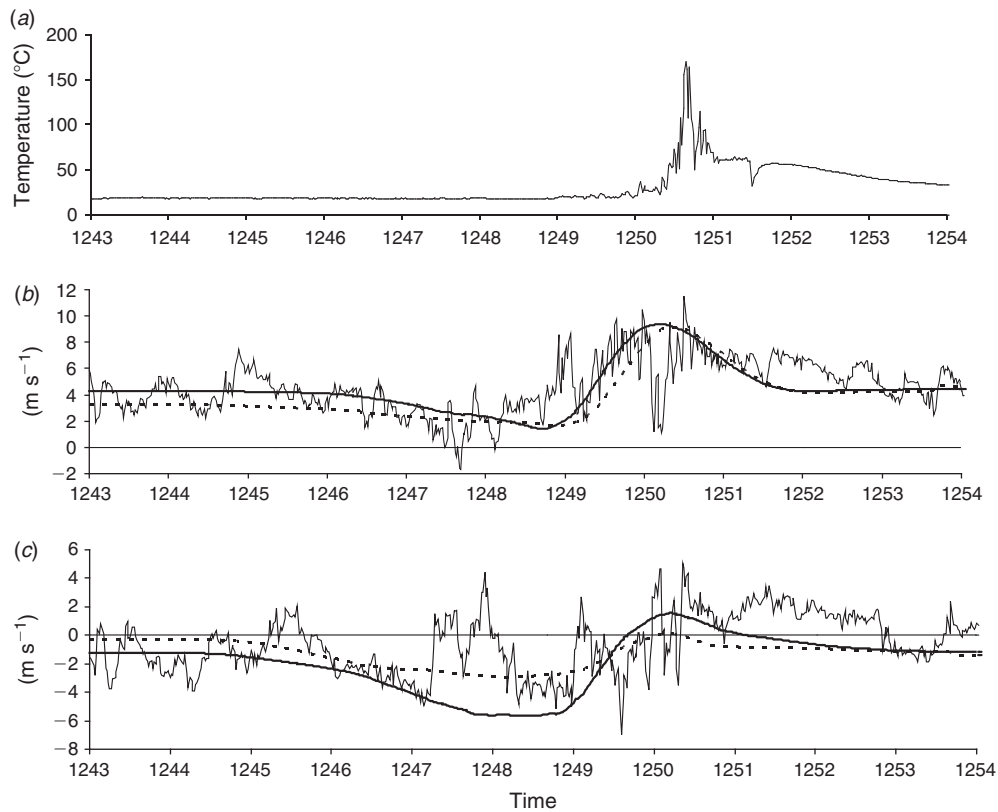


Fig. 6. Same as Fig. 5 but for the south tower.

One-second time-series of *u*- and *v*-component winds at the main tower are shown in Fig. 5. The *u*-component is defined as positive to the south in the direction of fire spread and the *v*-component is defined as positive to the east. The *u*-components (Fig. 5*b*) reversed direction at 1245:50 hours to blow from the south at -1.5 m s^{-1} , the reversal identified by Clements (2010) as a zone of convergence signalling the arrival of the plume. Wind gusts increased to $\sim 10 \text{ m s}^{-1}$ at 1246:30 hours, the time of fire passage (Fig. 5*a*). Then speeds declined to near ambient levels.

Two simulations, H125V25 (initialised with south tower ambient winds) and H150V20VW (initialised with main tower ambient winds), were selected for comparison with the observed main tower wind data because the average ROS from ignition to main tower approximately matched the observed fire spread rate (0.63 m s^{-1}).

Though the in-phase H125V25 *u*-component (solid line Fig. 5*b*), slowed from 3.97 m s^{-1} to 3.27 m s^{-1} at 1245:30 hours, there was insufficient time for the simulation winds at the main tower location to respond fully to the coupled fire-atmosphere pressure field during ramp-up. The *u*-component increased to 9.3 m s^{-1} at 1247:00 hours then declined to near ambient speeds thereafter. Run H150V20VW (dotted line), gave a better visual fit to the observations though the peak wind was phase-shifted by 10 s meaning the ROS was less than the observed ROS. The simulation produced an average ignition to tower ROS of 0.60 m s^{-1} .

The *v*-component time-series (Fig. 5*c*) was less useful for this study because it was not known exactly where the head of

the fire passed the towers. As the fire approached the main tower, the observed *v*-component time-series was characterised by increasing turbulence typical of a broad area of light and variable winds simulated ahead of a grassfire by Linn and Cunningham (2005). At 1245:50 hours, the time of plume passage identified by Clements (2010), the *v*-component shifted to blow mostly from the west with gusts to 6 m s^{-1} . The inference is that the tower was located within strong indraft along the right flank as the head passed just east of the tower. Both Rabbit Rules simulated fireheads passed just west of the main tower thus producing mean indraft from the east.

Simulations H125V25 and H150V20VW were again chosen for comparisons with 1-second time-series of *u*- and *v*-component winds at the south tower. As shown in Fig. 6*b*, H125V25 (solid line) was in phase with the observed *u*-component maximum equalling the observed ROS of 1.33 m s^{-1} calculated between the main and south towers. H150V20VW (dashed line), lagged by 10 s, produced a spread rate of 1.28 m s^{-1} .

Winds typically oscillated from 2 to 4 m s^{-1} until 1246:30 hours when a notable decline in speed culminated in a brief wind shift at 1247:35 hours (primary minimum) to blow from the south towards the fire. Then winds returned to northerly and speeds increased to a maximum of 8.7 m s^{-1} at 1249:00 hours followed by a secondary minimum of 2.1 m s^{-1} at 1249:27 hours and then a peak of 10.5 m s^{-1} at 1249:59 hours. The speed minimum of 1.1 m s^{-1} at 1250:13 hours was identified by Clements *et al.* (2007) as part of the circulation induced by the fire. The *u*-component peaked again at 11.5 m s^{-1} at 1250:30 hours followed by a gradual decline to ambient speeds.

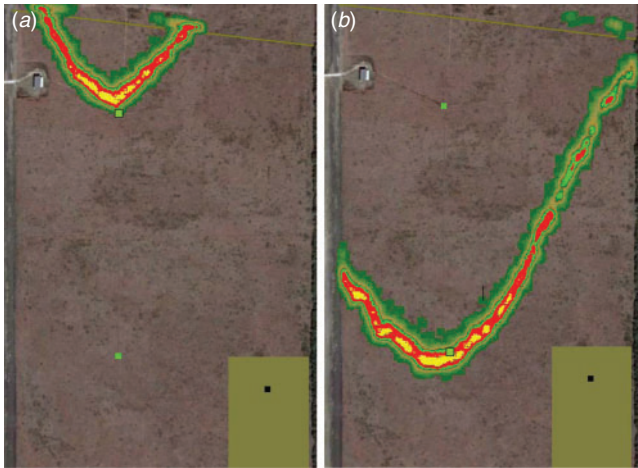


Fig. 7. From simulation H150V20VW. Fire approaches (a) the north tower at 1243:40 hours LST and (b) has just passed the south tower at 1251:40 hours LST.

The H125V25 u-component time-series (solid line) failed to decline to the primary speed minimum at 1247:35 hours. The speed minimum of 0.85 m s^{-1} occurred at 1248:46 hours as the observed u-component increased to the first peak. Then, from 1249:00 to 1251:00 hours, the simulated u-components approximated the observed wind components both in phase and magnitude (excepting the fire-induced circulation) and afterward returned to ambient speeds. The H150V20VW simulation shifted the phase of the speed maximum by 10 s thus reducing the average ROS by 0.05 m s^{-1} .

Given the observed fire spread rate and the period from passage of the primary speed minimum until passage of the fire (2:55 min), the primary wind minimum occurred 233 m ahead of the fire. But the temperature increase occurred during passage of the secondary minimum at 1249:14 hours (98 m ahead of the fire). Thus the secondary minimum fits the criteria for plume passage set by Clements (2010).

As noted, the v-component time-series (Fig. 5c) was less useful for this study because the location of the head was unknown when the fire passed the towers. With a few exceptions, the observed v-component blew from the east until shifting to blow from the west during passage of the fire. The inference is that the tower was located east of the head within strong flanking easterly winds as the flank approached. Then the v-component shifted to blow from the west as the tower was found in winds blowing towards the fire line from behind. Both Rabbit Rules simulations followed the same scenario.

Comparisons with FireFlux: fire line depth and fire intensity

Fire intensity is defined as the integral of the amount of fire (flame) over a unit area. In Rabbit Rules, fire intensity is the sum of the vigour (v_g) over a 130-m^2 area calculated internally in the model. Fig. 7a and 7b show for simulation H150V20VW the simulated fire line approaching the main tower (green square) at 1246:40 hours LST and just having passed the south tower at 1751.40 LST. The fire line depth is determined by ignition mechanics of the fire front in Rabbit Rules. Ignition is not along a solid line but rather over a zone of rasters as rabbits jump to

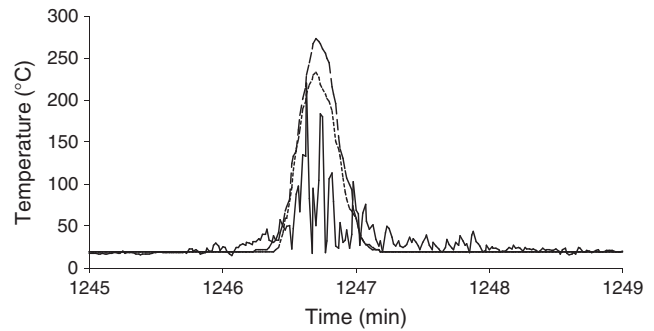


Fig. 8. A 4-min time-series of temperature at 2 m from the main tower. The dashed and solid lines show temperatures simulated by Rabbit Rules.

unburned fuel. The ignition zone is wider where winds blowing through the fire are faster – such as at the fire head. The fire line depth of the ‘intense’ (red and yellow) part of the fire line is 20 m and the depth of the entire line is 45 m.

Calculating fire line depth from temperatures observed at 2 m is complicated by non-fire temperature anomalies. Fig. 8 shows a 4-min subset of 2-m main tower temperature (black line) centred at the fire. Temperature rises before 1246:30 hours can be attributed to passage of hot gases within the plume being transported downwind ahead of the fire (Clements 2010). Above-ambient temperatures on the upwind side of the plume (after 1247:10 hours) may be explained by convective heat transport from fire-heated ground or residual smouldering. The residence time of fire (1246:30–1246:51 hours) (highest temperatures at the main tower) converts to a fire line width of 28 m for a ROS of 1.33 m s^{-1} . If less intense fire occurred through 1247:10 hours, the depth of the fire line would have been 53 m. These fire line dimensions compare favourably with those simulated by Rabbit Rules. The residence time of fire at the south tower was not calculated because of instrument malfunction after 1251:00 hours.

Temperature at 2 m at the main tower can be calculated during the passage of the fire line in Fig. 7a as follows. The heat release rate is estimated as 50% of the product of the mass of fuel consumed per unit time and the heat of combustion ($1.85 \times 10^7 \text{ J kg}^{-1}$) (Byram 1959) with the other 50% going into the heating of surrounding vegetation and ground surface. Clements *et al.* (2007) estimated the fuel loading as 1.08 kg m^{-2} . The total area burned in the simulations (Fig. 3) was calculated via Google Earth as $2.57 \times 10^5 \text{ m}^2$ and involved $\sim 580\,000$ rabbits. The fuel consumed per rabbit was 0.48 kg per rabbit. Furthermore, from Table 1, the average rabbit lifespan was 6 s. Therefore the heat release rate per rabbit was $Q = 7.4 \times 10^5 \text{ J s}^{-1}$ per rabbit.

The temperature difference between the plume air and ambient conditions at 2 m (ΔT_0), the mean plume vertical velocity (w_0) and the initial plume diameter (d_0) can be related to the heat of the fire (Mercer and Weber 2001) per rabbit by:

$$w_0 d_0^2 \Delta T_0 = \frac{4Q}{\pi C_p \rho} = 942 \quad (8)$$

in units of square metres per metre per second per kelvin per rabbit, where C_p is the specific heat ($\text{J kg}^{-1} \text{ K}^{-1}$) and ρ is the air density (kg m^{-3}). The unit of plume rise (flux) is defined as the

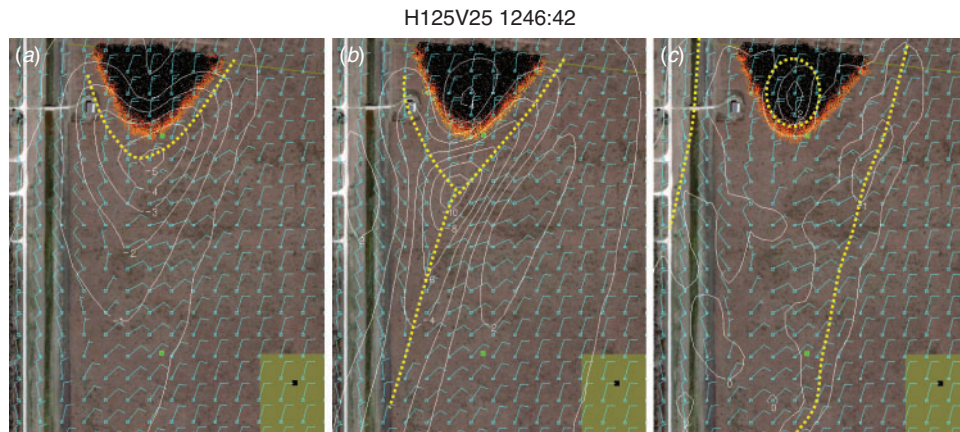


Fig. 9. Interface model winds on a 30-m grid for simulation H125V25 at 1246:40 hours with the following fields superimposed: (a) pressure anomaly, (b) divergence and (c) Rule FA2.

area unit of fire intensity, 130 m^2 ($d_0 = 12.8 \text{ m}$), over a vertical velocity of 2 m s^{-1} (Clements *et al.* 2007). Thus the temperature anomaly becomes $\Delta T_0 = 2.85 \text{ K}$ per rabbit. Multiplying by the number of rabbits per unit area as the fire line passed the main tower (Fig. 7a) and adding the 19°C ambient temperature yields the estimate for the time-series of plume temperature (dashed line) in Fig. 8. However, Clements *et al.* reported that the grass around the tower was mowed out to a distance of $\sim 5 \text{ m}$ from the base. The dotted line in Fig. 8 shows the estimated temperature time-series when Rabbit Rules was rerun with the area set as non-fuel.

Comparisons with other model: two-dimensional wind fields

Time-series of tower wind data are the only field measurements of wind near the fire taken during FireFlux. Windfields simulated by Rabbit Rules were compared with results from other models under the assumption that fundamental similarities exist among grassfires, and there should be found qualitative agreement with results from model simulations of other grassfires. Acceleration of winds through the fire line was also found by Clark *et al.* (1996) for a selection of ambient wind speeds. Their results placed the maximum wind $\sim 30 \text{ m}$ downwind from the fire line. Rabbit Rules collocated the maximum wind time-series with the observations at both towers (Figs 5, 6) placing the wind maximum just downwind from the fire line between the results from Clark *et al.* and those from (Linn and Cunningham 2005).

Turning of flank winds towards the front of the fire (Fig. 9a) was modelled by (Clark *et al.* 1996; Linn and Cunningham 2005; Cunningham and Linn 2007; Mell *et al.* 2007; Beezley *et al.* 2008). A convergence zone between flank winds and air accelerated through the fire (dotted line in Fig. 9b) formed 30 to 150 m ahead of the fire depending on the ambient wind speed (Clark *et al.* 1996). Greatest separation occurred where fastest winds were blowing through the head and near the deepest pressure anomaly (Fig. 9a). Divergence centres ahead and to the sides of the fire found by Clark *et al.* would be represented by draw-down Rule FA2 in Rabbit Rules (dotted lines in Fig. 9c).

Discussion and conclusions

This article has described Rabbit Rules, a free-agent cellular automata fire model, which represents fire spread by a set of

simple rules that can simulate non-linear processes not possible with empirical fire spread models yet is simpler and faster than full-physics fire models. In his review of FIRETEC, Sullivan (2009a) noted that a 200-s simulation on a 64-processor super-computer would take from 3.3 to 6.7 h to complete. A simulation of a 540-s (9-min) burn by Rabbit Rules for the FireFlux study took $\sim 5 \text{ min}$ on a desktop PC. However, the fire-rabbit analogy is not perfect and the model cannot reproduce exactly all physical processes.

Rabbit Rules has the capability to quickly test sensitivity to a range of fire and atmospheric parameters. It can be used to eliminate tests that potentially would return low value and to inform fire modellers of tests that likely would add to knowledge of fire behaviour or improve fire models. For example, tests are showing that Rule FA1 makes ROS dependent on length and shape of the fire line. Tests with and without Rule FA2 and using ambient winds with no vertical wind shear revealed that Rule FA2 slowed ROS by $\sim 10\%$. However, under extreme shear conditions, for example, 2 m winds equal to 5 m s^{-1} and 100 m winds equal to 20 m s^{-1} , Rule FA2 increased ROS by 25%.

Although designed for application with heterogeneous fuels distributed over complex terrain, no conclusions on the validity of the model can be drawn beyond the FireFlux study done with homogeneous fuels (tall grass) spread over flat ground. The study was done under prescribed fire conditions over a limited area. No studies to date have been done for wildfire spread over large landscapes and that can generate extreme conditions of fire-atmosphere coupling for which Rabbit Rules in its current configuration was not designed. Validation under these conditions is a subject for future study.

Furthermore, Rabbit Rules, being linked to the simple interface weather model, cannot simulate fully four-dimensional coupled fire and atmospheric phenomena such as feedbacks between plume and ambient environment that could under extreme conditions generate intense vertical circulations (including vortices) that could affect fire behaviour locally. Fire behaviour simulated by the CA fire model linked to a fully four-dimensional fluid dynamics model is a subject for future study.

Conceptually, other more complex formulations may be equally valid, or provide equally valuable but different understanding of the fire-rabbit relationship. Perhaps the salient

contribution of this paper is to challenge readers to further explore the CA-free agent approach subject to constraints imposed by their ecosystems.

Acknowledgements

Dr Craig Clements is acknowledged for providing FireFlux experiment data for Rabbit Rules validation. Dr Scott Goodrick, Dr Yonqiang Liu and Dr J. J. O'Brien provided stimulating discussions during preparation of the manuscript. Dr Warren Heilman provided wind data measured by Doppler sodar. This study was funded through the National Fire Plan 01.SRSA5.

References

- Achtemeier GL (2003) 'Rabbit Rules' – an application of Stephen Wolfram's 'New Kind of Science' to fire spread modeling. In 'Fifth Symposium on Fire and Forest Meteorology', 16–20 November 2003, Orlando, FL. (American Meteorological Society: Boston, MA)
- Achtemeier GL (2005) Planned Burn–Piedmont. A local operational numerical meteorological model for tracking smoke on the ground at night: model development and sensitivity tests. *International Journal of Wildland Fire* **14**, 85–98. doi:10.1071/WF04041
- Adou JK, Billaud Y, Brou DA, Clerc J-P, Consalvi J-L, Fuentes A, Kaiss A, Nmira F, Porterie B, Zekri L, Zekri N (2010) Simulating wildfire patterns using a small-world network model. *Ecological Modelling* **221**, 1463–1471. doi:10.1016/J.ECOLMODEL.2010.02.015
- Andrews PL (2008) BehavePlus fire modeling system, version 4.0: variables. USDA Forest Service, Rocky Mountain Research Station, Report RMRS-GTR-213WWW. (Fort Collins, CO)
- Andrews PL, Bevins CD, Seli RC (2005) BehavePlus fire modeling system, version 3.0: User's Guide. USDA Forest Service, Rocky Mountain Research Station, Report RMRS-GTR-106WWW Revised. (Ogden, UT)
- Beezley JD, Chakraborty S, Coen JL, Douglas CC, Mandel J, Vodacek A, Wang Z (2008) Real-time data driven wildland fire modelling. *Lecture Notes in Computer Science* **5103**, 46–53. doi:10.1007/978-3-540-69389-5_7
- Berjak SG, Hearne JW (2002) An improved cellular automaton model for simulating fire in a spatially heterogeneous Savanna system. *Ecological Modelling* **148**, 133–151. doi:10.1016/S0304-3800(01)00423-9
- Bouchaud J-P, Georges A (1990) Anomalous diffusion in random media: models, statistical mechanisms and physical realizations. *Physics Reports* **195**, 127–293. doi:10.1016/0370-1573(90)90099-N
- Byram GM (1959) Combustion of forest fuels. In 'Forest Fire control and Use'. (Ed. KP Davis) pp. 155–182. (McGraw Hill: New York)
- Clark TL, Jenkins MA, Coen J, Packham D (1996) A coupled atmospheric-fire model: convective Froude number and dynamic fingering. *International Journal of Wildland Fire* **6**, 177–190. doi:10.1071/WF9960177
- Clarke KC, Olsen G (1996) Refining a cellular automaton model for wildfire propagation and extinction. In 'GIS and Environmental Modeling: Progress and Research Issues'. (Eds MF Goodchild, LT Steyaert, BO Parks, C Johnston) pp. 333–338. (Wiley: Hoboken, NJ)
- Clarke KC, Brass JA, Riggan PJ (1994) A cellular automaton model of wildfire propagation and extinction. *Photogrammetric Engineering and Remote Sensing* **60**(11), 1355–1367.
- Clements CB (2010) Thermodynamic structure of a grass fire plume. *International Journal of Wildland Fire* **19**, 895–902. doi:10.1071/WF09009
- Clements CB, Zhong S, Goodrick S, Li J, Potter BE, Bian X, Heilman WE, Charney JJ, Perna R, Jang M, Lee M, Patel M, Street S, Aumann G (2007) Observing the dynamics of wildland grass fires: FireFlux – a field validation experiment. *Bulletin of the American Meteorological Society* **88**, 1369–1382. doi:10.1175/BAMS-88-9-1369
- Cunningham P, Linn RR (2007) Numerical simulation of grass fires using a coupled atmosphere–fire model: dynamics of fire spread. *Journal of Geophysical Research – Atmospheres* **112**, D05108. doi:10.1029/2006JD007638
- Hernández Encinas A, Hernández Encinas L, White SH, Martín del Rey A, Rodríguez Sánchez G (2007) Simulation of forest fire fronts using cellular automata. *Advances in Engineering Software* **38**, 372–378. doi:10.1016/J.ADVENGSOFT.2006.09.002
- Flakes GW (2000) 'The Computational Beauty of Nature: Computer Explorations of Fractals, Chaos, Complex Systems, and Adaptation.' (MIT Press: Cambridge, MA)
- Grell GA, Dudhia J, Stauffer DR (1994) A description of the fifth-generation Penn State/NCAR mesoscale model (MM5). National Center for Atmospheric Research, Technical Note NCAR/TN-3921STR. (Boulder, CO)
- Hargrove WW, Gardner RH, Turner MG, Romme WH, Despain DG (2000) Simulating fire patterns in heterogeneous landscapes. *Ecological Modelling* **135**, 243–263. doi:10.1016/S0304-3800(00)00368-9
- Karafyllidis I, Thanailakis A (1997) A model for predicting forest fire spreading using cellular automata. *Ecological Modelling* **99**, 87–97. doi:10.1016/S0304-3800(96)01942-4
- Linn RR (1997) Transport model for prediction of wildfire behavior. Los Alamos National Laboratory, Scientific Report LA13334-T. (Los Alamos, NM)
- Linn RR, Cunningham P (2005) Numerical simulations of grass fires using a coupled atmosphere–fire model: basic fire behavior and dependence on wind speed. *Journal of Geophysical Research* **110**, D13107. doi:10.1029/2004JD005597
- Linn RR, Harlow FH (1998) FIRETEC: a transport description of wildfire behavior. In 'Second Symposium on Forest and Fire Meteorology', 11–16 January 1998, Phoenix, AZ. (Eds FM Fujioka, DW Goens) pp. 14–19. (American Meteorological Society: Boston, MA)
- Linn RR, Winterkamp J, Edminster C, Colman JJ, Smith WS (2007) Coupled influences of topography and wind on wildland fire behaviour. *International Journal of Wildland Fire* **16**, 183–195. doi:10.1071/WF06078
- Mell W, Jenkins MA, Gould J, Cheney P (2007) A physics-based approach to modeling grassland fires. *International Journal of Wildland Fire* **16**, 1–22. doi:10.1071/WF06002
- Mercer GN, Weber RO (2001) 'Fire Plumes in Forest Fires: Behavioral and Ecological Effects.' (Eds EA Johnson, K Miyaniishi) pp. 225–256. (Academic Press: New York)
- Metzler R, Klafter J (2000) The random walk's guide to anomalous diffusion: a fractional dynamics approach. *Physics Reports* **339**, 1–77. doi:10.1016/S0370-1573(00)00070-3
- Rothermel RC (1972) A mathematical model for predicting fire spread in wildland fuels. USDA Forest Service, Intermountain Research Station, Research Paper INT-115. (Ogden, UT)
- Skamarock WC, Klemp JB, Dudhia J, Gill DO, Barker DM, Wang W, Powers JG (2005) A description of the advanced research WRF Version 2. National Center for Atmospheric Research, Technical Note, NCAR/TN-468+STR. (Boulder, CO)
- Sullivan AL (2009a) Wildland surface fire spread modeling, 1990–2007: 1. Physical and quasi-physical models. *International Journal of Wildland Fire* **18**, 349–368. doi:10.1071/WF06143
- Sullivan AL (2009b) Wildland surface fire spread modeling, 1990–2007: 2. Empirical and quasi-empirical models. *International Journal of Wildland Fire* **18**, 369–386. doi:10.1071/WF06142
- Sullivan AL, Knight IK (2004) A hybrid cellular automata/semi-physical model of fire growth. In 'Proceedings of the Seventh Asia–Pacific Conference on Complex Systems', 6–10 December 2004, Cairns, Qld. (Eds R Stoner, Q Han, W Li) pp. 64–73. Available at <http://www.dar.csiro.au/css/research/sullivan/complex2004%20sullivan%20and%20knight.pdf> [Verified 12 September 2012]
- Yassemi S, Dragicevic S, Schmidt M (2008) Design and implementation of an integrated GIS-based cellular automata model to characterize forest fire behaviour. *Ecological Modelling* **210**, 71–84. doi:10.1016/J.ECOLMODEL.2007.07.020